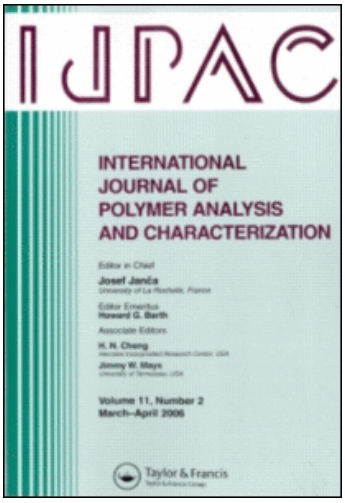

International Journal of Polymer Analysis and Characterization
Publication details, including instructions for authors and subscription information:
http://www.informaworld.com/smpp/title~content=t713646643

Peak Characterization and Errors in Dynamic Mechanical Analysis of Polymer Blends

Charles E. Chaffey[a]
[a] Chemical Engineering and Applied Chemistry, University of Toronto, Toronto, ON, Canada

To cite this Article Chaffey, Charles E.(1999) 'Peak Characterization and Errors in Dynamic Mechanical Analysis of Polymer Blends', International Journal of Polymer Analysis and Characterization, 5: 1, 1 — 19
To link to this Article: DOI: 10.1080/10236669908014170
URL: http://dx.doi.org/10.1080/10236669908014170

Int. J. Polym. Anal. Charact.,
1999 Vol. 5, pp. 1–19
Reprints available directly from the publisher
Photocopying permitted by license only

Peak Characterization and Errors in Dynamic Mechanical Analysis of Polymer Blends*

CHARLES E. CHAFFEY

Chemical Engineering and Applied Chemistry, University of Toronto, 200 College Street, Toronto, ON, Canada M5S 3E5

(Received 8 October 1997; In final form 8 June 1998)

Viscoelastic behavior is advantageously displayed using the relaxation spectrum, because its distinct peaks correspond to processes centered at definite relaxation times. Quantitative characterization then becomes possible using parameters for strength, location, spread, and rate of decay, in the mathematical functions representing the peaks. Use of symmetric bell-shaped functions that occur in statistical theory makes a practical method possible, for solving the generally ill-posed inverse problem of finding the relaxation spectrum, using spreadsheet software. The starting data are observations of complex modulus from dynamic mechanical analysis (DMA). Time-temperature superposition allows the result to be displayed as a temperature sweep, at some reference time. From data in the literature, referred to a time of 1000 s, a poly(*n*-octyl methacrylate) fraction can be characterized with three peaks, at 55°C, −42°C and −56°C, and a commercial polystyrene with two peaks, at 122°C and 108°C. Published data for rubbery copolymers and their blends with isotactic polypropylene give spectra with one peak for the terminal zone, at 21°C to 35°C, depending on the material, when referred to time 1 s. For the immiscible blend an additional peak appears at 93°C, corresponding to phase separation; from its location one can estimate 50 Pa for the ratio of interfacial tension to droplet radius. Random errors in the DMA data degrade the precision of the method, so that typically a 5% noise level in the complex modulus would cause peaks separated by 8°C to become merged.

Keywords: Relaxation spectrum; Dynamic mechanical analysis; Polymer blends

* Presented at the 10th International Symposium on Polymer Analysis and Characterization, (ISPAC-10), University of Toronto, Canada, August 10–13, 1997.

INTRODUCTION

Dynamic mechanical analysis (DMA) is a versatile technique for characterizing the behavior, over a range of temperature, of polymers and their blends. Its value can be enhanced by displaying its results as a relaxation spectrum H. To obtain H from the raw data of DMA, which are values of the complex modulus G^*, one must invert the integral equation

$$G^*(\omega) = G' + iG'' = \int_{-\infty}^{\infty} H(\tau) \frac{i\omega\tau}{1 + i\omega\tau} \, d(\ln \tau), \tag{1}$$

where ω is angular frequency and τ is relaxation time. Because Equation (1) gives $G^*(\omega)$ as an expected value over the probability density $H(\tau)$, it shows that relaxation processes at many time scales τ add to the observed G^* at any one frequency ω. Thus the relaxation spectrum $H(\tau)$ gives a direct measure of the strength of viscoelastic relaxation at each time scale τ, and a plot of $H(\tau)$ against τ has peaks that show the regions where relaxation processes are concentrated. The peaks, and also the regions of roughly constant slope on a logarithmic plot of H, can be identified with the characteristic zones of viscoelastic behavior, such as the glassy zone, the glass transition, the rubbery plateau, and the terminal zone, in single-phase polymers and blends.[1] An additional peak appears at long τ, due to phase separation, in immiscible, two-phase blends.[2] These peaks in the single function H will be more distinct than the features seen in plots against ω of the two components of G^*, namely, inflections in G' and extrema in G''. The contrast between DMA data from materials having good and poor qualities in applications, cited in their brochures by DMA instrument manufacturers (for example, Rheometrics, TA Instruments), should also be clearer when the relaxation spectrum H is used.

Because H at one τ contributes to G^* over all frequencies ω, there can be many quite different functions $H(\tau)$ that give almost the same $G^*(\omega)$ by Equation (1). The inverse problem of finding $H(\tau)$ from $G^*(\omega)$ is thus ill-posed.[3] Traditionally, H is calculated by an approximate method such as those of Williams and Ferry[1] or Tschoegl,[3] which work well because $H(\tau)$ is a slowly varying function of τ. Numerically calculated spectra have further been decomposed into separate peaks, the areas of which correspond to the strengths of

different viscoelastic processes.[1] More recent methods for computing H, such as the maximum entropy method,[4] consider how the errors in $G^*(\omega)$ are distributed. A new adaptive-robust minimax algorithm makes no assumption of error bounds, and also takes into account non-Gaussian outliers.[5] High accuracy is obtained from regularization with quadratic programming, used with G' data at low ω and G'' data at high ω.[6] Like the early approximations, these methods too give numerical values of $H(\tau)$ at discrete values of τ that can be displayed graphically, but which do not yield a limited set of parameters suitable for characterization.

A different strategy is to represent $H(\tau)$ analytically by a slowly varying function having a small number of parameters. Early examples are the box and wedge spectra.[1] More recently, the BSW spectrum of Baumgärtel, Schausberger, and Winter, descending and ascending wedges, has been introduced[7] for monodisperse amorphous polymers; the mixing rules for bidisperse systems have also been determined.[8] Because the corners on the graphs of these functions are physically unrealistic and absent from numerically calculated spectra, smoother functions seem to be advantageous.[3] The present research will study how results of DMA can be displayed by a relaxation spectrum H that consists of a few symmetric bell-shaped peaks. In practice, DMA experiments are quite often carried out as temperature sweeps; accordingly, the calculated spectra are shown using temperature as independent variable. This has the advantage of characterizing the relaxations by the temperatures at which they occur. Finally, the possible errors in this method are discussed.

THEORY

In general, a spectrum is found by observing the response of a sample to an excitation, which is scanned over a range of an independent variable x such as frequency or temperature. Typically the response has a small baseline magnitude except at special values of the scanned variable, at which the response rises to give peaks on the spectrum. Because random fluctuations spread the peaks out from being perfectly sharp and narrow, the response is appropriately modeled, as a function of the scanned variable, by one of the probability densities

arising in statistical theory. Two normalized symmetric density functions, which are described and tabulated in standard statistics texts[9] are used here.

The Gaussian or normal probability density function[3] is

$$n(x;\mu,\sigma) = \frac{1}{(2\pi)^{1/2}\sigma}\exp\left[-\frac{1}{2}\frac{(x-\mu)^2}{\sigma^2}\right], \tag{2}$$

where x is the random variable; the mean μ locates the center of the peak on the x scale, and the standard deviation σ measures the spread of the peak. This function is also useful for modeling secondary (β) relaxations at temperatures below the glass transition,[10] and stress relaxation of the amorphous and crystalline zones of solid isotactic polypropylene.[11] The second density function used is the Student t density (or Pearson Type VII distribution) defined in terms of the standardized random variable $t=(x-\mu)/\sigma$ by

$$f(t;\nu) = \frac{\Gamma(\nu+1)/2}{\Gamma(\nu/2)(\pi\nu)^{1/2}}\left(1+\frac{t}{\nu}\right)^{-(\nu+1)/2}, \tag{3}$$

where ν (the number of degrees of freedom) indicates the rate of decay of the function $f(t;\nu)$ as x differs more from μ. When ν is small $f(t;\nu)$ drops off gradually, but for large ν, $f(t;\nu)$ decreases abruptly. As $\nu\to\infty$ (effectively for $\nu\geq 100$), $f(t;\nu)\to n(t;0,1)$. It is this quality of gradual decay that makes the Student t density so important in its usual statistical application.

The variable x was identified as the logarithmic relaxation time: $x=\log\tau$ (τ in seconds; $\log\equiv\log_{10}$). A relaxation spectrum $H(\tau)$ containing N peaks was expressed by

$$H(\tau) = \sum_{j=1}^{N} H_j(\tau),$$

where

$$H_j(\tau) = G_j n(\log\tau;\mu_j,\sigma_j),$$

or

$$H_j(\tau) = G_j f\left(\frac{\log\tau - \mu_j}{\sigma_j}; \nu_j\right),$$

G_j (with units of modulus) being the strength or intensity of the relaxation for peak j. In this study, the number N of peaks was between 1 and 3. Spreadsheet software was then employed to calculate $\log G'$ and $\log G''$ as functions of $\log\omega$ for given parameters G_j, μ_j, σ_j and ν_j, with the trapezoidal rule used for the integration.

In the spreadsheet (Quattro Pro for Windows 5.0, Borland International Inc., 1993), the top 9 rows were reserved for general purposes, such as for constants, parameters and headings. Rows 10–200 were used for calculations; in them column A held 191 values of $\log\omega$ or $-\log\tau$ running from −4.0 to 15.0 in steps of 0.1:

$$\log\omega_k = -\log\tau_k = -4.0 + 0.1k, \quad \text{for } k = 0 \text{ to } 190.$$

The row index was $k+10$. Column B held $\omega_k = 1/\tau_k = 10^{-4.0+0.1k}$. J columns were used for $H_j(\tau_k)$, with their sum $H(\tau_k)$ in column H. To calculate G', the real part of Equation (1)

$$G' = \int_{-\infty}^{\infty} \frac{H(\tau)}{1 + 1/\omega^2\tau^2}\, \mathrm{d}(\ln\tau),$$

was integrated by the trapezoidal rule with 190 panels. The sum of the terms except the first and last was given by

$$K_k = \sum_{l=1}^{189} \frac{H(\tau_l)}{1 + \tau_l^{-2}/\omega_k^2}.$$

The cell at column K and row $k+10$ held K_k as a formula; its code, for $k=0$ for example, was @SUM(H$11..H$199/(1+B$11..B$199^2/B10^2)). The code makes use of the two interpretations of column B, ω_k and $1/\tau_k$. Copying the formula from row 10, to rows 11 through 200, automatically changed the reference from B10 to the correct row index. The trapezoidal integration was completed as

$$G'(\omega_k) = \frac{1}{2}\left[\frac{H(\tau_0)}{1 + \tau_0^{-2}/\omega_k^2} + 2K_k + \frac{H(\tau_{190})}{1 + \tau_{190}^{-2}/\omega_k^2}\right](0.1 \ln 10),$$

coded as 0.5*(H$10/(1 + (B$10/B10)^2) + 2*K10 + H$200/(1 + (B$200/B10)^2))*C$5. Cell C5 held 0.1 ln 10, the step size of 0.1 multiplied by ln 10, to convert $\log_{10}$ to ln.

The calculation of the loss modulus G'' was analogous:

$$G'' = \int_{-\infty}^{\infty} \frac{H(\tau)}{\omega\tau + 1/\omega\tau}\, \mathrm{d}(\ln\tau), \quad L_k = \sum_{l=1}^{189} \frac{H(\tau_l)}{\omega_k/\tau_l^{-1} + \tau_l^{-1}/\omega_k},$$

@SUM(H$11..H$199/(B10/B$11..B$199 + B$11..B$199/B10)),

$$G''(\omega_k) = \frac{1}{2}\left[\frac{H(\tau_0)}{\omega_k/\tau_0^{-1} + \tau_0^{-1}/\omega_k} + 2L_k + \frac{H(\tau_{190})}{\omega_k/\tau_{190}^{-1} + \tau_{190}^{-1}/\omega_k}\right](0.1 \ln 10),$$

0.5*(H$10/(B10/B$10 + B$10/B10) + 2*L10 + H$200/(B10/B$200+ B$200/B10))*C$5.

With calculated and observed $\log G'$ and $\log G''$ displayed in a graph window, the parameters G_j, μ_j, σ_j and ν_j were varied until the calculated and observed values matched fairly closely. This procedure could be started with $G_j = G''$, $\mu_j = -\log\omega$ of peak j, and $\sigma_j = 1$, $\nu_j = 30$. Increasing μ_j moved the calculated maxima in G' and G'' to lower ω; increasing G_j raised G' and G''; and increasing σ_j or decreasing ν_j made the changes in G' and G'' more gradual. Agreement between calculated and observed $\log G'$ and $\log G''$ was measured by the percentage root-mean-square (rms) deviations d' and d'' defined by

$$d' = \left[\frac{\sum(\log G'(\text{observed}) - \log G'(\text{calculated}))^2}{n_{\text{data}}}\right]^{1/2} \times 100\%, \qquad (4)$$

and analogously for d'', summation being over all n_{data} data points. For each peak in turn, the parameters G_j, μ_j, σ_j and ν_j were finally adjusted systematically to reduce d' and d'', until about two significant figures in the parameters were determined. However, peak locations were not reported as μ_j, but as the antilogarithm 10^{μ} with units of time, which placed the peaks on the actual time scale.

When time-temperature superposition[1] is valid, temperature T can be used instead of relaxation time τ as the independent variable. The

relaxation spectrum H can accordingly be displayed as a function of T. Superposition requires that $H(\tau,T) = H(\tau/a_T, T_0)$, where τ/a_T is the temperature-shifted relaxation time, with a_T being the shift factor for the reference temperature T_0. Now let T be the temperature at which the relaxation spectrum has this same value at a reference relaxation time τ_0: $H(\tau_0, T) = H(\tau/a_T, T_0)$. To obtain an explicit formula for T from this implicit equation, an expression for a_T is needed. One which is widely used is the Williams–Landel–Ferry (WLF) equation

$$\log a_T = \frac{-c_1(T - T_0)}{c_2 + T - T_0},$$

with the WLF parameters c_1 and c_2. Setting the temperature-shifted relaxation time τ/a_T equal to τ_0/a_T with variable T gives

$$\log(\tau/a_T) = \log \tau_0 + \frac{c_1(T - T_0)}{c_2 + T - T_0},$$

which can be solved for T to yield

$$T = T_0 - c_2 \frac{\log \tau_0 - \log(\tau/a_T)}{c_1 + \log \tau_0 - \log(\tau/a_T)}. \tag{5}$$

For systems that are more fluid, at temperatures much above the glass transition, a_T is represented well by the Arrhenius equation

$$\log a_T = \frac{E}{R \ln 10}\left(\frac{1}{T} - \frac{1}{T_0}\right),$$

where E is the apparent activation energy, and R is the gas constant, $8.3145\,\mathrm{J\,K^{-1}\,mol^{-1}}$. Analogously to the derivation of Equation (5), equating τ/a_T to τ_0/a_T and solving for variable T gives

$$T = \left[\frac{\log \tau_0 - \log(\tau/a_T)}{E/R \ln 10} + \frac{1}{T_0}\right]^{-1}. \tag{6}$$

In Equations (5) and (6), $c_1 > 0$, $c_2 > 0$ and $E > 0$; these inequalities cause a change to a shorter τ_0 to result in a higher calculated T. Thus choosing a shorter reference time will displace the features of the

relaxation spectrum to higher temperatures; their shape will also be altered. To locate the relaxation peaks on the temperature scale, temperatures T_μ are introduced, defined by Equations (5) or (6) with $\log \mu$ substituted for $\log(\tau/a_T)$.

RESULTS

As examples, these methods have been applied to DMA data in the literature for some representative systems.

System 1. Poly(*n*-octyl Methacrylate)[1]

This data set extends over 15.5 decades of temperature-shifted time. A satisfactory fit was obtained from a relaxation spectrum $H(\tau)$ having three Student t peaks, Equation (3), with parameters given in Table I. On the logarithmic plot of G', G'' against ωa_T (Figure 1(a)), the curves of the recovered G', G'' agree with the data best near the extrema in G''. Transformation to temperature as independent variable by Equation (5) shows the dependence of the relaxation processes on T (Figure 1(b)), at the arbitrarily chosen reference relaxation time $\tau_0 = 1000$ s. Here the WLF parameters are $T_0 = 100°C$, $c_1 = 7.60$, $c_2 = 227.3°C$.[1] After this nonlinear transformation the maxima in H are located by T_μ (Table I), and the peaks are no longer symmetric. Values of H, calculated by the Williams–Ferry method,[1] plotted as +, × on Fig. 1b, agree closely with the middle Student t peak but diverge

TABLE I Parameters in Equations (2) and (3), and rms deviations for five polymer and blend systems

System	*Strength G*	*Location* 10^μ (s)	*Location* T_μ, (°C)	*Spread* σ	*Decay* ν	d', d'' (%)
1	1.9×10^5 dyn/cm^2	10	55	1.0	4	5.5, 7.8
	1.4×10^9 dyn/cm^2	2.5×10^{-10}	−42	1.0	9	
	5.5×10^9 dyn/cm^2	3.2×10^{-14}	−56	0.5	30	
2	6.5×10^5	0.63	122	1.0		—, 2.6
	1.0×10^6	3.2×10^{-3}	108	0.5		
3	3.9×10^4 Pa	8×10^{-3}	34	0.6		2.3, 3.2
	6.5×10^4 Pa	10^{-4}	−32	1.0		
	1.8×10^7 Pa	3.2×10^{-12}	−143	1.7		
4	3.3×10^4 Pa	6.3×10^{-3}	29	0.55		5.4, 2.9
5	43 Pa	0.1	93	1.2		2.3, 1.5
	5.4×10^4 Pa	4×10^{-3}	21	0.6		

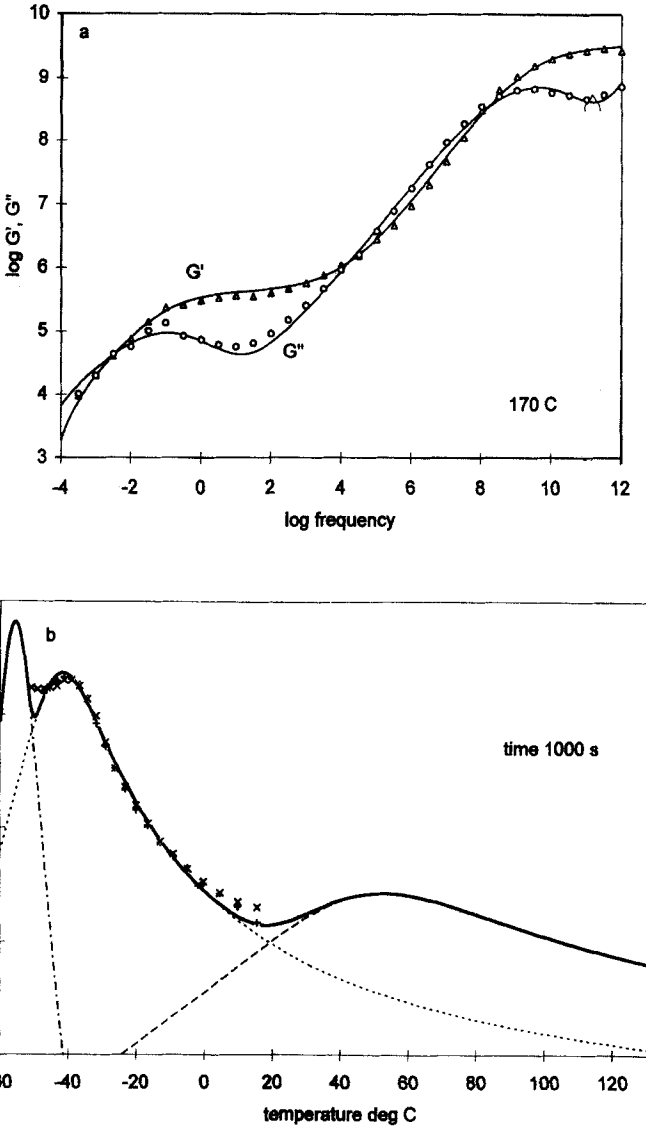

FIGURE 1 Data for system **1**, a poly(*n*-octyl methacrylate) fraction.[1] (a) Double logarithmic plot of complex modulus G^* against temperature-shifted frequency ωa_T. Δ, observed G'; $\bigcirc$, observed G''; curves, G' and G'' recovered from the relaxation spectrum $H(\tau)$ with symmetric peaks. (b) H plotted against temperature T for a reference relaxation time $\tau_0 = 1000$ s: lower curves, individual peaks; upper curve, their summation giving H; + and $\times$, points of the relaxation spectrum calculated in the original reference from G' and G'', respectively.

at the ends of their range. If the reference time is shortened to $\tau_0 =$ 100 s, the maxima of the three Student t peaks are displaced upwards; for example, $T_{\mu 1}$ is shifted from 55°C to 74°C.

System 2. Commercial Polystyrene

One of the data sets of Elster and Honerkamp[4] (their Figure 6) is a master curve of G'' for a commercial polystyrene from measurements at 160°C to 280°C (G' is not reported[4]). On Figure 2(a) these data are shown together with the curves of G' and G'' recovered from a relaxation spectrum $H(\tau)$ having two Gaussian peaks, Equation (3). The peaks are characterized in Table I; the units of G are those of the reference.[4] To change to T as independent variable (Figure 2(b)) by Equation (5), WLF parameters were calculated from tabulated values at the glass transition, using Ferry's Table 11-II and Equations (24) and (25) of section B, chapter 11.[1] At $T_0 = 160$°C, inferred from the data,[4] $c_1 = 5.877$, $c_2 = 107.5$°C; again $\tau_0 = 1000$ s. Elster and Honerkamp use the maximum entropy method to estimate $H(\tau)$. Their values

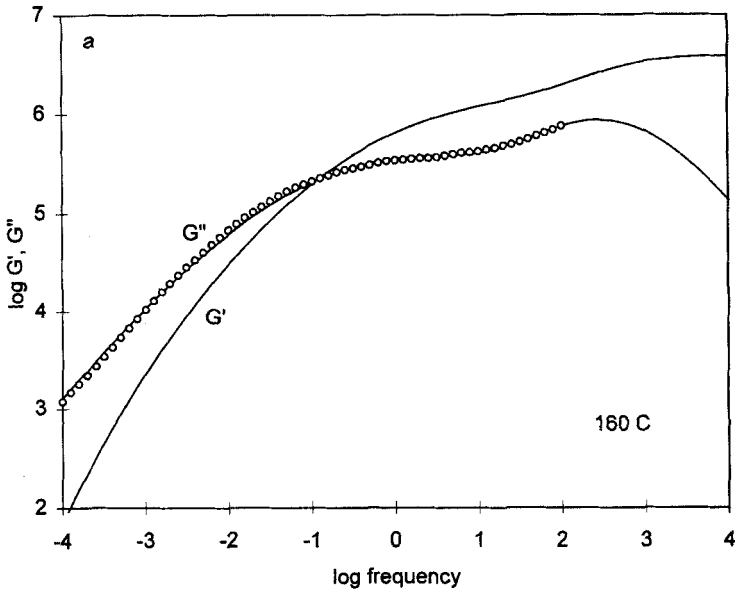

FIGURE 2(a)

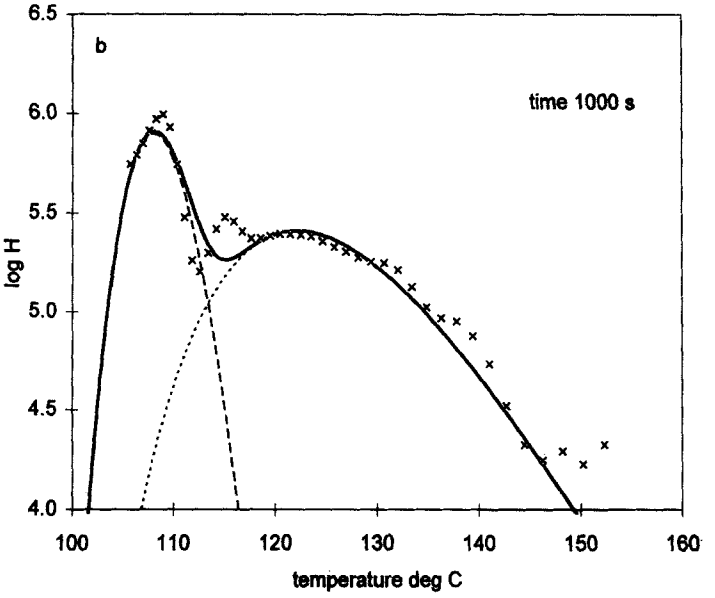

FIGURE 2(b)

FIGURE 2 Data for system **2**, a commercial polystyrene,[4] plotted as in Figure 1.

of H, shown without the error estimates as $\times$ on Fig. 2(b), fluctuate more than the H of the present model, in which only two relaxation processes suffice to reproduce G'' with the low d'' of 2.6%.

System 3. Rubbery Copolymer

Yamaguchi *et al.* have recently published an extensive rheological study[12] of polymers and their blends. Those authors' Figure 1 gives master curves of G' and G'', reduced to 170°C, for a rubbery copolymer of 43 mol % ethylene and 57% 1-hexene. They are replotted here in Figure 3(a), together with recovered values calculated from a relaxation spectrum $H(\tau)$ having three Gaussian peaks with parameters given in Table I. Equation (6) with $E = 40.5\,\text{kJ/mol}$[12] is used to change the independent variable to T, against which H is plotted in Figure 3(b). The reference relaxation time $\tau_0 = 1$ s. As T increases from about −65°C, H has a broad box-like region extending to 70°C. The method proposed here decomposes this feature into two bell-shaped

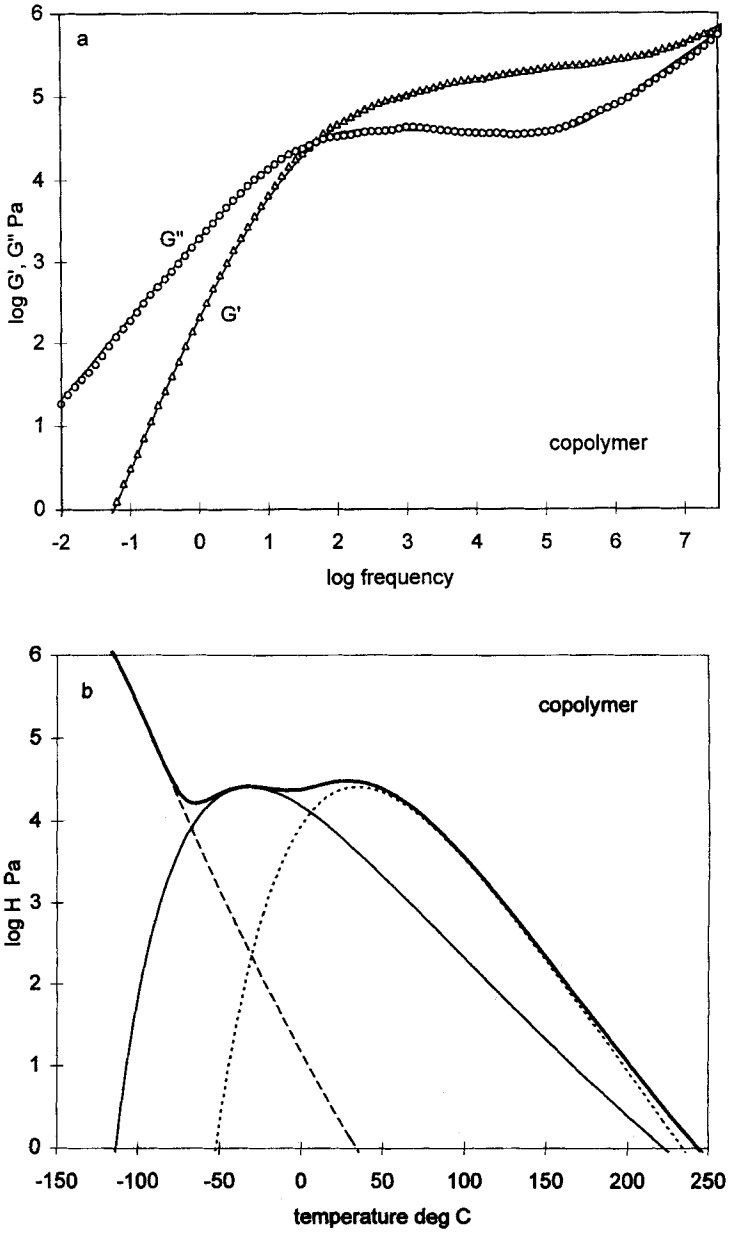

FIGURE 3 Data for system 3, a rubbery copolymer,[12] plotted as in Figure 1, for a reference relaxation time $\tau_0 = 1$ s.

peaks, which cannot be resolved by inspection (Figure 3(b)). In order of increasing τ or T, they may be identified with the rubbery plateau and the terminal zone, respectively. The present method also provides numerical values for both the strength G, and the location 10^{μ} on the time scale, of these two viscoelastic behaviors (Table I).

System 4. Miscible Blend of Polypropylene and Rubbery Copolymer

Figures 2 and 4 of Yamaguchi *et al.*[12] report $G^*(\omega)$ and $H(\tau)$ data for two blends. System **4**, which is 75% by mass isotactic polypropylene (i-PP) and 25% the rubbery copolymer of system **3**, a miscible blend, shows the usual terminal zone in which $\log G'$ has slope 2 at low ωa_T (Figure 4(a)). Over the range of frequency for which measurements were possible, G' and G'' are adequately recovered from a single Gaussian relaxation (Figure 4(b); Table I). The calculated crossover of G' and G'' (Figure 4(a)) is displaced down in frequency compared to the observations. Agreement would be improved if a second peak in H

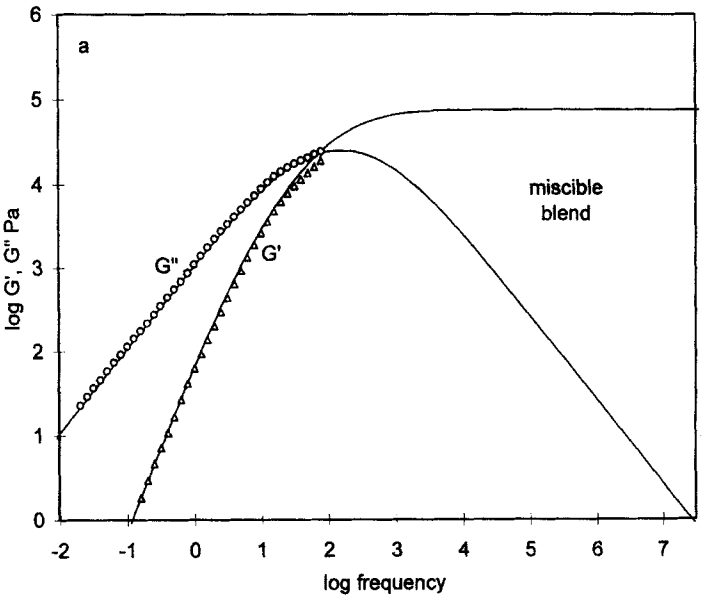

FIGURE 4(a)

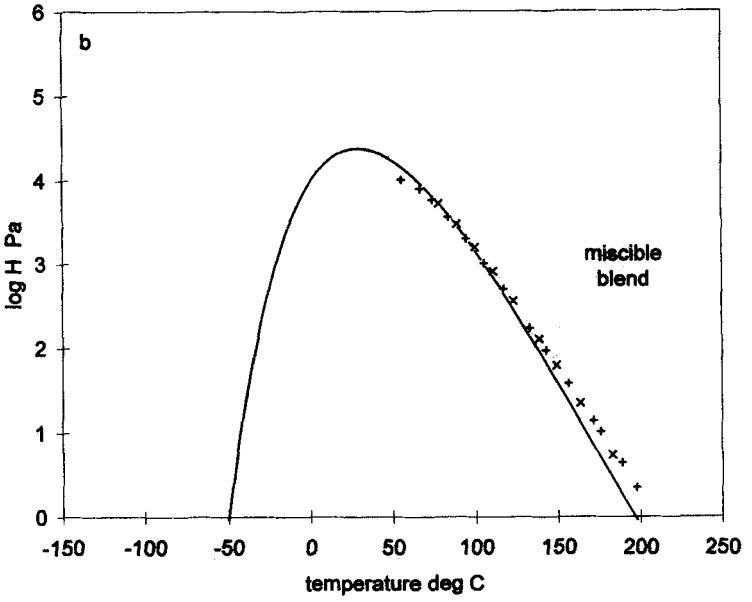

FIGURE 4(b)

FIGURE 4 Data for miscible blend 4 of isotactic polypropylene with rubbery copolymer,[12] plotted as in Figure 3.

was added at low temperatures, but since it would lie outside the range of the observations its parameters would not be meaningful.

System 5. Two-phase Blend of Polypropylene and Rubbery Copolymer

A blend of 75% by mass i-PP, and 25% copolymer of 70 mol% ethylene and 30% 1-hexene, separates into two phases. The plot of $\log G'$ against $\log \omega a_T$ has a slope greater than 2 at low ωa_T[12] (Figure 5(a)). Two Gaussian peaks are required in the relaxation spectrum H (Figure 5(b); Table I). The one at larger τ or T, due to phase separation, occurs at a relaxation time $10^{\mu} = 0.1$ s. Substitution of this value into Equation (6) of Gramespacher and Meissner[2] yields a ratio of interfacial tension to droplet radius of 50 Pa (given by $2\,\mathrm{mN\,m^{-1}}/40\,\mu\mathrm{m}$, for example). A comparable relaxation at high temperature, attributable

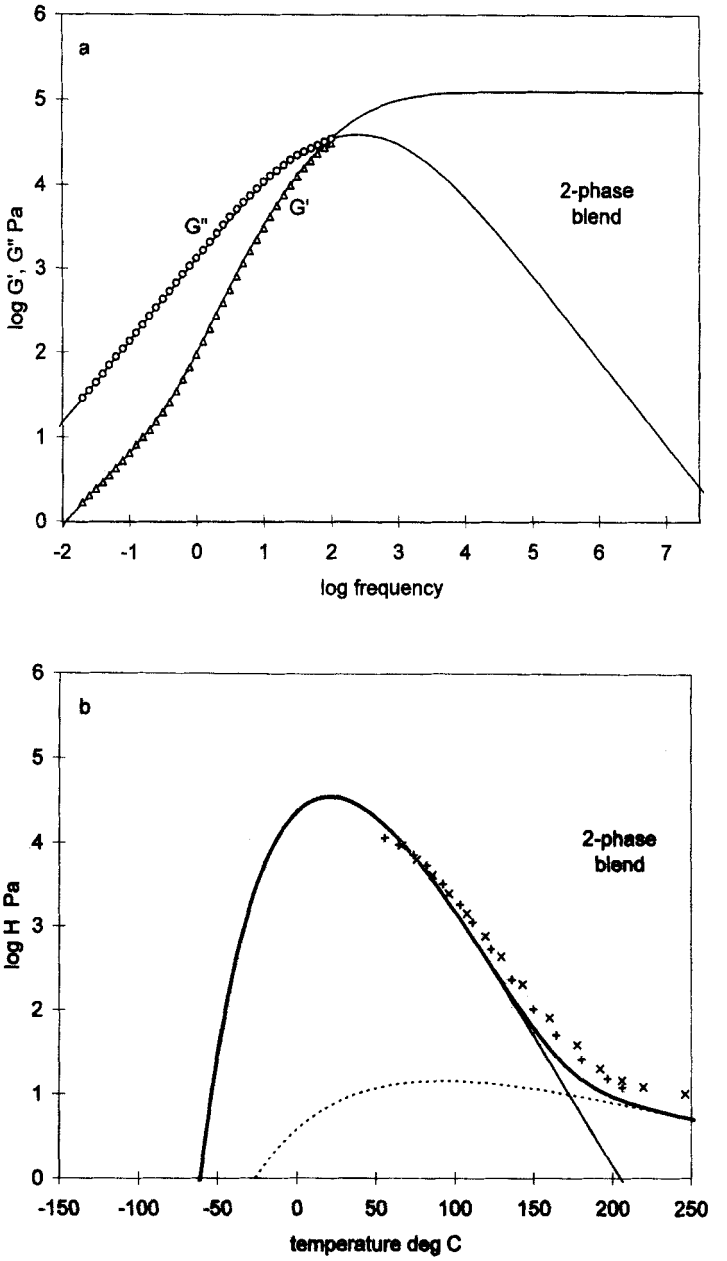

FIGURE 5 Data for two-phase blend **5** of isotactic polypropylene with rubbery copolymer,[12] plotted as in Figure 3.

to an interface between two phases, has been identified in a series of polyurethane blends.[13] For the blends **4** and **5** here, Equation (6) was used for T, with $E = 40.2\,\text{kJ/mol}$[12] and $\tau_0 = 1\,\text{s}$. The values of H calculated using the Tschoegl equations by Yamaguchi *et al.*,[12] shown as $+$, $\times$ on Figures 4(b) and 5(b), indicate slightly broader relaxations than the Gaussian peaks.

For these systems, the precision of recovery of $\log G'$ and $\log G''$, as measured by d' and d'', Equation (4), is within 3.2%, with two exceptions. The relaxations in system **1**, which extend over wider ranges in frequency, need the additional parameter ν_j in the Student t function, Equation (3), to attain 7.8% precision. For system **4**, the H with just one peak also gives reduced precision in $\log G'$. Figures 1(b), 2(b), 3(b) and 5(b) show that with multiple peaks, only one tail of each peak contributes significantly to H, so that the tail that is not significant can be taken as symmetric to the significant tail. In general, these relaxation spectra H built from bell-shaped peaks, symmetric in the frequency domain, represent the viscoelastic behavior with good precision.

DISCUSSION

Some test calculations were done to learn about possible errors in characterizing relaxations by the present method. The following procedure examined the small difference in complex moduli $G^*(\omega)$ from a spectrum $H(\tau)$ having two sharp peaks close together, and from one having a single broader relaxation. For the former H, a line spectrum was used. It was from two parallel Maxwell elements with equal moduli $\frac{1}{2}G$, and with relaxation times $\alpha\tau$, τ/α, where α was a predetermined multiplier, so that

$$G^*(\omega) = \tfrac{1}{2}G[\mathrm{i}\alpha\omega\tau/(1 + \mathrm{i}\alpha\omega\tau) + \mathrm{i}\omega(\tau/\alpha)/(1 + \mathrm{i}\omega\tau/\alpha)].$$

This was modeled by a single Gaussian peak, Equation (2), with modulus G and location $10^{\mu} = \tau$. Its spread σ was then determined so as to minimize $(d' + d'')/2$, Equation (4). Finally, the temperature dependence and τ_0 were chosen to illustrate the result; $\alpha\tau$ was selected to give $T = 108°\text{C}$ when substituted in Equation (5), and then a temperature separation ΔT was calculated as the difference between the T

corresponding to τ/α and 108°C. Figure 6 is a plot of a relative standard deviation $(d' + d'')/2G$ against ΔT. In practice, random noise will contribute to d' and d'' when actual data are analyzed. It is expected that the ordinate of Figure 6 also indicates the level of noise, for which it is impossible to resolve relaxations having temperatures T_μ closer than the ΔT plotted on the abscissa. For example, one would make the error of failing to distinguish two peaks that are 8°C apart when the relative standard deviation is greater than 5%, for the conditions of system **2**. Similar calculations show that at higher temperatures the minimum separation between just resolvable relaxations increases. Alternatively, at the same noise level, the analysis might erroneously split a single broad relaxation into two narrow ones.

Errors will also be caused by imperfect time-temperature superposition. The resulting scatter in the master curves of G' and G'' will degrade the calculated H like random noise. Lack of precision in the shift factor a_T also affects the peaks, especially their locations T_μ.

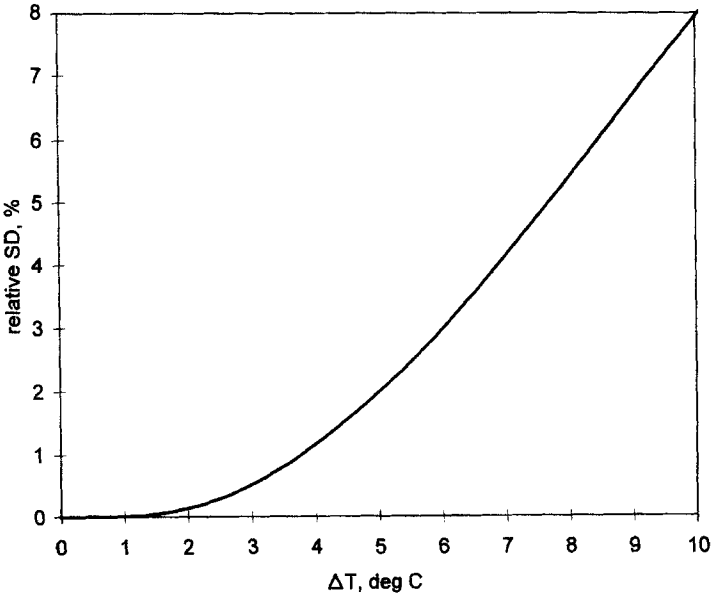

FIGURE 6 Precision in G^* data, expressed as standard deviation relative to the glassy modulus, needed to resolve a peak at a temperature higher by ΔT from one at 108°C, for the conditions of Figure 2.

Thus with Equation (5), a unit increase in the WLF parameter c_1 or an 8°C decrease in c_2 shifts the peaks upwards in T by 4°C.

For the systems analyzed here, the master curves had minimal scatter, indicating low noise and good superposition. Since the relaxation peaks (Table I) are widely separated in τ or temperature T, and the deviations d', d'' are small, it does not appear that any peaks have been either separated or merged incorrectly.

CONCLUSIONS

The complex modulus G^* of a viscoelastic polymer or blend, as measured by dynamic mechanical analysis, can be represented well by a relaxation spectrum H having a few symmetric, bell-shaped peaks. Two or three such peaks are enough to span the range of relaxation times or temperatures from the glass transition to the terminal zone, for the systems from the literature studied here. The Gaussian or normal density function, multiplied by a strength parameter G, can describe the shape of a peak over a moderately wide range of relaxation time; its mean μ and standard deviation σ are quantitative measures of the location and spread of the relaxation. When the data have a wider range of relaxation time, the Student t density function is useful since it has an additional parameter ν indicating the decay of the peak away from its maximum. The method yields numerical values for these parameters which thus can characterize the polymer viscoelasticity at a particular temperature T_0. Transformation to temperature T as independent variable, possible because of time–temperature superposition, allows the spectrum to be displayed as a temperature sweep, with relaxations assigned to characteristic temperatures T_μ, for a reference time τ_0.

Random noise in the measured complex modulus G^* makes the peaks in H appear lower and wider, and causes errors in distinguishing two narrow nearby relaxations from a single broader one. In a typical case, a noise level of 5% in relative standard deviation would cause two relaxations separated by 8°C in temperature not to be resolved.

The method is straightforward to implement using spreadsheet software, and it should enhance the ability to characterize polymer materials quantitatively using DMA.

References

[1] Ferry, J.D. (1970). *Viscoelastic Properties of Polymers*; 2nd ed.; pp. 34, 64, 71, 82, 91, 402, 642–3 (John Wiley: New York).
[2] Gramespacher, H. and Meissner, J. (1992). *J. Rheol.*, **36**, 1127.
[3] Tschoegl, N.W. (1989). *The Phenomenological Theory of Linear Viscoelastic Behavior*; pp. 170, 191, 342 (Springer-Verlag: Berlin).
[4] Elster, C. and Honerkamp, J. (1992). *J. Rheol.*, **36**, 911.
[5] Yanovsky, Yu.G., Basistov, Yu.A. and Siginer, D.A. (1996). *Int. J. Eng. Sci.*, **34**, 1221.
[6] Ramkumar, D.H.S., Caruthers, J.M., Mavridis, H. and Shroff, R. (1997). *J. Appl. Polym. Sci.*, **64**, 2177.
[7] Baumgärtel, M., Schausberger, A. and Winter, H.H. (1990). *Rheol. Acta*, **29**, 400.
[8] Jackson, J.K. and Winter, H.H. (1995). *Macromolecules*, **28**, 3146.
[9] Walpole, R.E. and Myers, R.H. (1993). *Probability and Statistics for Engineers and Scientists*; 5th ed.; pp. 141, 227 (Prentice-Hall: Englewood Cliffs).
[10] Dutta, N.K. and Edward, G.H. (1997). *J. Appl. Polym. Sci.*, **66**, 1101.
[11] Flores, R. and Perez, J. (1995). *Macromolecules*, **28**, 7171.
[12] Yamaguchi, M., Nitta, K.-H., Miyata, H. and Masuda, T. (1997). *J. Appl. Polym. Sci.*, **63**, 467.
[13] Rao, Q. and Yao, S. (1997). *J. Appl. Polym. Sci.*, **64**, 2067.